PREDICTION OF SHACKLE MOTION HANGED FROM A JIB TOP OF CRANE BARGE BY A COUPLING NUMERICAL MODEL OF THREE MOTIONS

YOSHINOSUKE KURAHARA, M. Eng.
Researcher, Coastal and Ocean Engineering Group,
Research and Development Center, TOA CORPORATION
1-3 Anzen-cho, Tsurumi-ku, Yokohama City, Kanagawa, 230-0035, Japan.
E-mail: y_kurahara@toa-const.co.jp

MASAHIDE TAKEDA, P.E.Jp (Civil Eng.), Dr. Eng.
Group Manager, Coastal and Ocean Engineering Group,
Research and Development Center, TOA CORPORATION

HAJIME MASE, Dr. Eng.
Technical Adviser, TOA CORPORATION
Research Professor, Disaster Prevention Research Institute, Kyoto University

Keywords: hook, shackle, crane barge, oscillation prediction, oscillation control, numerical model

1. Introduction

Crane barge, shown in *Fig. 1*, is an indispensable vessel for marine construction works and various cargo handling operations at sea. When handle cargoes using a crane barge, the hull and suspended loads are usually shaken due to waves. The prediction and control of the shaking or oscillation are extremely important from the viewpoint of safety operation, increase the effective working days, accurate construction work and so on. To predict the oscillation, Nojiri and Mita (1980) have developed a computation method for coupled motions of crane barge and suspended load based on a linear theory. They have found that the developed method is able to explain the characteristics of coupled motions by comparing the predictions with the experimental results using a 1/50 scale model of 2500 tons crane barge.

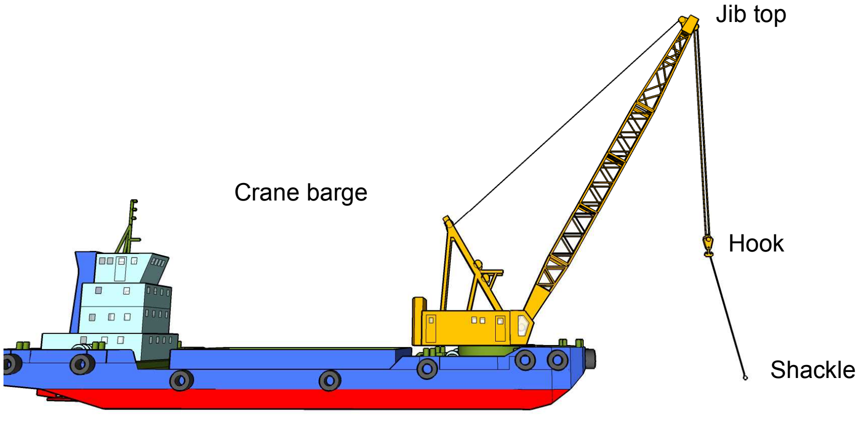

Figure 1: Sketch of crane barge

Before lifting the suspended loads, slinging work has to be done; that is hanging the load on hook using a hooking tool such as wire ropes. In the case of crane barge, a U-shaped shackle is attached to the tip of a wire hanging from the hook in advance. Then the shackle is connected to the lifting lug welded onto the load for slinging work. The shackle weight for a load of 100 tons is from 150 to 250 kg for the crane work when using a large crane barge. In the open ocean, these large shackles swing with large amplitudes as shown in *Fig. 2*. Even in calm sea conditions where the significant wave height is 0.5 m or less, the workers cannot catch the shackles and cannot continue the crane work. In this way, the operation rate of construction work is greatly affected depending on whether the slinging can be done or not.

Therefore, since the shaking prediction of shackle is important, we developed and proposed a numerical model for coupling of double pendulum motions of hook, shackle and ship motions based on a linear theory, especially to predict the motion of shackle on a crane barge.

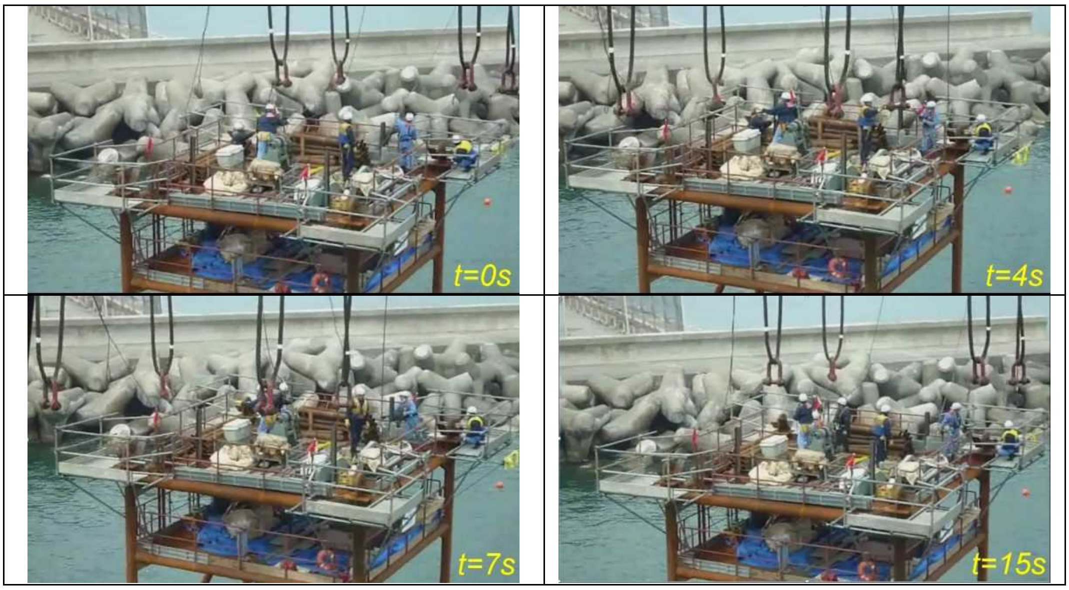

Figure 2: Swinging shackles during slinging work

2. Numerical Model

2.1. Coupling model of motions and coordinate system

The numerical model proposed here to predict the motion of crane barge is a radiation/diffraction panel model based on the linear theory. The model considers the interaction between surface waves and crane barge is based on a three-dimensional panel method.

It is assumed in this model that waves and hull motions are small and the infinite domain is analyzed by the linear theory. The fluid is assumed to be non-viscous, incompressible and irrotational motion being described by a velocity potential. A crane barge is modeled as a box-shaped three-dimensional rigid body.

In the Cartesian coordinate system (X, Y, Z), as shown in *Fig. 3*, the X and Y axes are set on the still water surface and the Z axis is in the vertical downward direction, and the center of the hull is set as the origin O. The translational motion in each axis direction is denoted as X_1 for surge, X_2 for sway, X_3 for heave, and the rotational motion around each axis is denoted as X_4 for roll, X_5 for pitch and X_6 for yaw. The hook and the shackle are suspended from the jib top located at (l_x, l_y, l_z). A hook's x direction motion in the XZ plane is denoted as X_7, shackle's x direction motion as X_8, in the

YZ plane X_9 is for hook's y direction motion and X_{10} for shackle's y direction motion. Thus, the motion modes of crane barge, hook and shackle are denoted as X_j (j = 1 to 10). The β is the angle between the incident direction wave and the positive X axis as defined in *Fig. 3*.

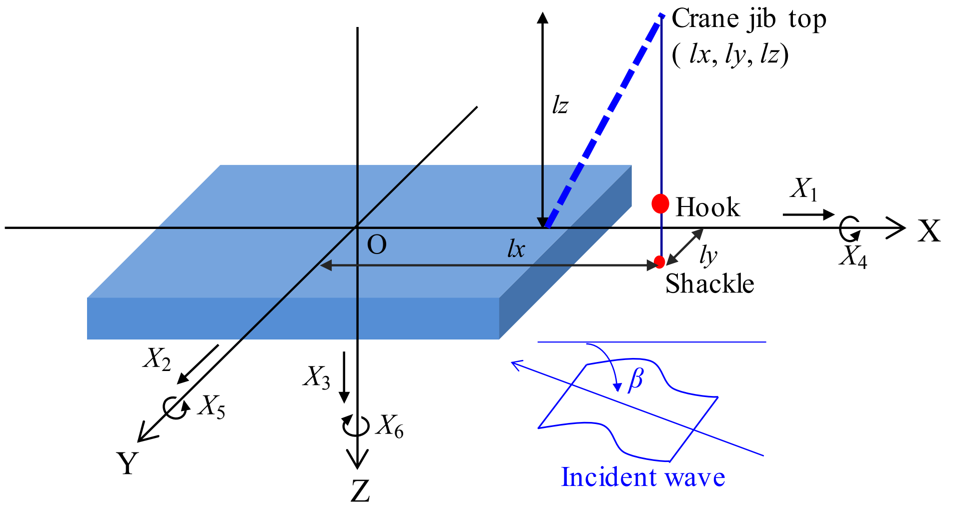

Figure 3: Coordinate system

2.2. Governing equation

2.2.1. Double pendulum motions of hook and shackle

The hook and shackle of a crane barge show double pendulum motions fixed at a jib top. The motions of the hook and shackle are caused by motion of the jib top. The motions of hook and shackle in the XZ plane are shown in *Fig. 4*. The length of the hanging from the jib top to hook is l_7, the length of the hanging from hook to shackle l_8, and the length of hanging from the jib top to shackle l (=l_7+l_8). The hook weight is m_1, shackle weight m_2, and the total hanging weight m (=m_7+m_8). In the XZ plane, the horizontal displacement and swing angle of hook are X_7 and φ_7, those of shackle X_8 and φ_8, and the horizontal displacement of the jib top $X_{j\text{-}xz}$. Relationship between the horizontal movement distance of the hook and the shackle and the swing angle is expressed by the formula of Eq. (1).

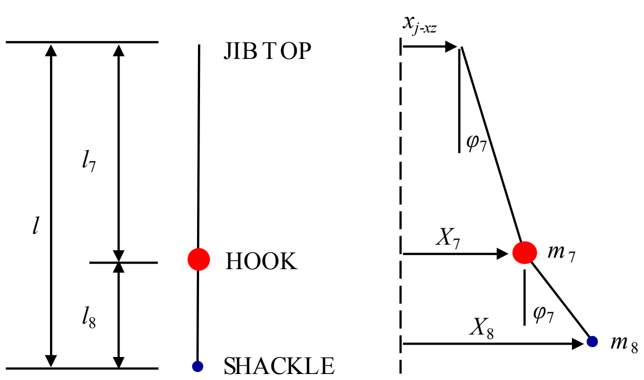

Figure 4: Double pendulum model consist of hook and shackle

$$\begin{cases} X_7 = X_{j-xz} + l_7\varphi_7 \\ X_8 = X_{j-xz} + l_7\varphi_7 + l_8\varphi_8 \end{cases} \quad (1)$$

The motions of the hook and shackle in the XZ plane can be expressed by the Lagrange equation of Eq. (2). The determinants $\boldsymbol{A}$, $\boldsymbol{B}$, $\boldsymbol{C}$ and $\boldsymbol{D}$ are given by Eq. (3).

$$\boldsymbol{A}\begin{Bmatrix}\ddot{X}_7\\ \ddot{X}_8\end{Bmatrix}+\boldsymbol{B}\begin{Bmatrix}\dot{X}_7\\ \dot{X}_8\end{Bmatrix}+\boldsymbol{C}\begin{Bmatrix}X_7\\ X_8\end{Bmatrix}=\boldsymbol{D} \tag{2}$$

$$\left.\begin{aligned}
\boldsymbol{A} &= \begin{bmatrix} m_7 & 0\\ 0 & m_8\end{bmatrix}\\
\boldsymbol{B} &= \begin{bmatrix} c_7 m_7\sqrt{2g/l_7}+c_8 m_8\sqrt{2g/l_8} & -c_8 m_8\sqrt{2g/l_8}\\ -c_8 m_8\sqrt{2g/l_8} & c_8 m_8\sqrt{2g/l_8}\end{bmatrix}\\
\boldsymbol{C} &= \begin{bmatrix} m_7\, g/l_7+m_8\, g/l_8 & -m_8\, g/l_8\\ -m_8\, g/l_8 & m_8\, g/l_8\end{bmatrix}\\
\boldsymbol{D} &= \begin{bmatrix} (m_7\, g/l_7)X_{j-xz}+\left(c_7 m_7\sqrt{2g/l_7}\right)\dot{X}_{j-xz}\\ 0\end{bmatrix}
\end{aligned}\right\} \tag{3}$$

where c_7 and c_8 are the damping coefficients related to the damping force term proportional to the horizontal displacement speed. The displacement of the jib top can be expressed by Eq. (4) derived from the movement of crane barge.

$$X_{j-xz}=X_1+l_z X_5-l_y X_6 \tag{4}$$

Similarly, the motion of hook and shackle in the YZ plane can be calculated by the simultaneous differential equations of hook X_9 and shackle X_{10}. In the YZ plane, it is sufficient to give the displacement $X_{j\text{-}yz}$ of the jib top as Eq. (5) from the movement of crane barge.

$$X_{j-xz}=X_1+l_z X_5-l_y X_6 \tag{5}$$

2.2.2. Analysis method of hull motion

Generally, wave-exciting force (Froude-Krylova force + diffraction force), radiation force, and static restoring force act on a floating body moving in waves. In addition to these forces, a coupled force acts on the jib top of crane barge as a dynamic reaction force due to the double pendulum motions of hook and shackle. Therefore, the equation of motions of crane barge is expressed as Eq. (6).

$$\sum_{j=1}^{6} m_{ij}\ddot{X}_j(t)=F_{Di}(t)+F_{Ri}(t)+F_{Si}(t)+F_{Ci}(t) \tag{6}$$

where $F_{Di}(t)$: the wave-exciting force, $F_{Ri}(t)$: the radiation force, $F_{Si}(t)$: the static restoring force, $F_{Ci}(t)$: the coupled force by hook and shackle double pendulum motions.

In this model, wind drag force, flow drag force, mooring force and other environmental external forces are not considered. Wave-exciting force and radiation force are calculated from three-dimensional velocity potential using the three dimensional singularity distribution method (*e.g.* Tsutsumi *et al.*, 1974, or Inglis and Price, 1980). The static restoring force is calculated from the balance between the center of hull's gravity and buoyancy forces.

1) F_{Di} : Wave-exciting force

As shown in *Fig. 5*, the force (wave-exciting force and radiation force) that the hull of crane barge receives from the water surface is calculated by adding the fluid fluctuating pressure $p(P,\ t)$ acting on the point $P(x_p, y_p, z_p)$ in the total surface area S_H. As shown in Eq. (7), the fluid fluctuation pressure of waves is calculated by the speed potential with a normal vector n_i.

$$F_{Di}(t) = -\int_{S_H} p_D(P,t)n_i(P)dS_P = \rho \int_{S_H} \frac{\partial}{\partial t}\Phi_D(P,t)n_i(P)dS_P \tag{7}$$

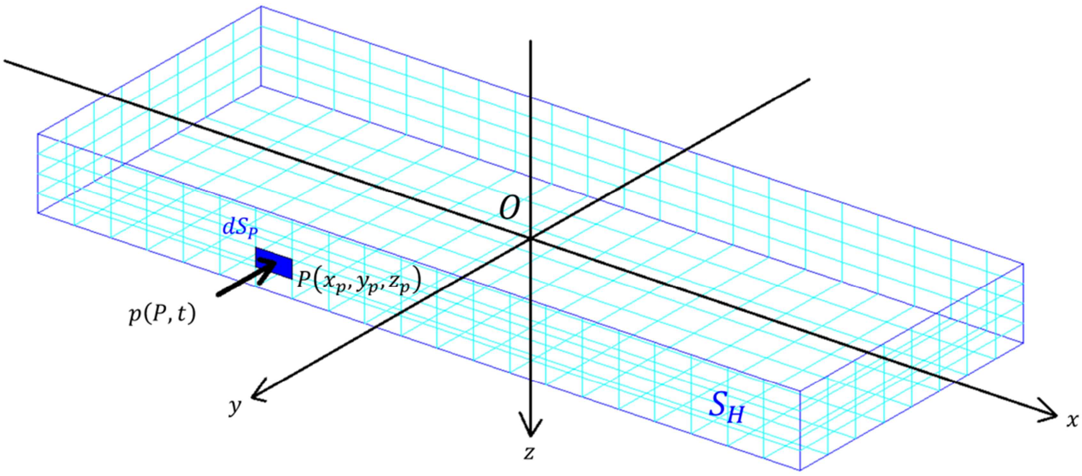

Figure 5: Discretization of hull under the water surface to a microscopic plane element

The velocity potential $\Phi_D(P,t)$ related to wave-exciting force is given by Eq. (8); $\Phi_D(P,t)$ is the sum of the incident wave velocity potential $\Phi_0(P,t)$ and the velocity potential $\Phi_7(P,t)$ of the fluid dispersion resulting from the hull reflection disturbance.

$$\Phi_D(P,t) = \Phi_7(P,t) + \Phi_0(P,t) \tag{8}$$

2) F_{Ri} : Radiation force

Similarly, the radiation force is expressed as Eq. (9) using the velocity potential.

$$F_{Ri}(t) = -\int_{S_H} p_R(P,t)n_i(P)dS_P = \rho \int_{S_H} \frac{\partial}{\partial t}\Phi_R(P,t)n_i(P)dS_P \tag{9}$$

The velocity potential $\Phi_R(P,t)$ of the radiation force is the sum of velocity potential $\Phi_j(P,t)$ caused by waves consisting of motion mode ($j = 1$ to 6) of the hull of crane barge, described as Eq. (10).

$$\Phi_R(P,t) = \sum_{j=1}^{6} \Phi_j(P,t) \tag{10}$$

The velocity potential $\Phi_j(P,t)$ fluctuates with time. Specifically, it is calculated from Eq. (11) by the convolution operation of the impulse velocity potential $\Delta\Phi_j(P,t)$ by an unit velocity and the motion speed $\dot{X}_j(t)$ from the past to present time t as follows:

$$\Phi_j(P,t) = \int_{-\infty}^{t} \Delta\Phi_j(P,t-\tau)\dot{X}_j(\tau)d\tau \tag{11}$$

Impulse velocity potential $\Delta\Phi_j(P,t)$ by an unit velocity is calculated by Eq. (12) (Takagi and Arai, 1996) bellow.

$$\Delta\Phi_j(P,t) = \Omega_j(P)\delta(t) + \Gamma_j(P,t)H(t) \tag{12}$$

where, $\delta(t)$: the delta function ($\delta(t)=0$ for $t\neq 0$, $\delta(t)=\infty$ for $t=0$), $H(t)$: Heaviside function ($H(t)=1$ for $t\geq 0$, $H(t)=0$ for $t<0$), $\Omega_j(P)$: the velocity potential of turbulent wave in the vicinity of the hull, $\Gamma_j(P,t)$: the velocity potential of divergent wave from the hull in far of the hull.

Therefore, the radiation force is given by Eqs. (13) and (14).

$$\begin{aligned} F_R(t) &= \rho\sum_{j=1}^{6}\int_{S_H}\Omega_j(P)n_i(P)dS_p\ddot{X}_j(t) + \int_{-\infty}^{t}\int_{S_H}\frac{\partial}{\partial t}\Gamma_j(P,t-\tau)n_i(P)dS_p\dot{X}_j(\tau)d\tau \\ &= \sum_{j=1}^{6}\left[-m_{ij}(\infty)\ddot{X}_j(t) - \int_{-\infty}^{t}\mathrm{L}_{ij}(t-\tau)\dot{X}_j(\tau)d\tau\right] \end{aligned} \tag{13}$$

$$\left.\begin{aligned} m_{ij}(\infty) &= -\rho\int_{S_H}\Omega_j(P)n_i(P)dS_p \\ L_{ij}(t) &= -\rho\int_{S_H}\frac{\partial}{\partial t}\Gamma_j(P,t-\tau)n_i(P)dS_p \end{aligned}\right\} \tag{14}$$

where, $m_{ij}(\infty)$: the additional mass coefficient at $\omega=\infty$ (generally not zero), $L_{ij}(t)$: the memory influence function of fluid force.

3) F_{Si} : static restoring force

As shown in Eqs. (15) and (16), the static restoring force is expressed using the modes $ij = 33$, 35, 53, 44, and 55. The other modes of C_{ij} are zero.

$$F_{Si}(t) = \sum_{j=1}^{6} C_{ij}X_j(t) \tag{15}$$

$$\left.\begin{aligned} C_{33} &= \rho g A_W \\ C_{35} = C_{53} &= \rho g \int_{S_H} x_p dx_p dy_p \\ C_{44} &= \rho g \nabla \overline{GM_B} \\ C_{55} &= \rho g \nabla \overline{GM_L} \end{aligned}\right\} \tag{16}$$

where, A_W is the area of waterline surface, $\overline{GM_B}$ the horizontal meta center height, $\overline{GM_L}$ the vertical meta center height, ∇ the displacement, as shown in *Fig. 6*.

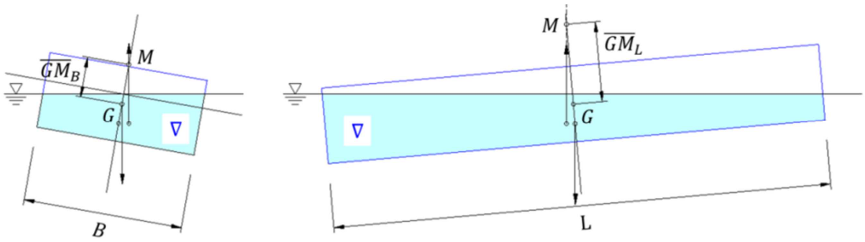

Figure 6: Meta center height appeared in Eq. (6)

4) F_{Ci} : Coupled force by hook and shackle motions

The coupled force due to the double pendulum motions of hook and shackle act on the jib top of crane barge. The coupled force is expressed by Eq. (17).

$$F_{Ci}(t) = \boldsymbol{M}\{\ddot{X}_1(t) \quad \ddot{X}_2(t) \quad \cdots \quad \ddot{X}_{10}(t)\}^{\mathrm{T}} \tag{17}$$

$$\boldsymbol{M} = \begin{bmatrix} m & 0 & 0 & 0 & ml_z & -ml_y & m_7 & m_8 & 0 & 0 \\ 0 & -m & 0 & -ml_z & 0 & -ml_x & 0 & 0 & -m_7 & -m_8 \\ 0 & 0 & 0 & 0 & 0 & 0 & 0 & 0 & 0 & 0 \\ 0 & ml_z & 0 & -ml_z{}^2 & 0 & ml_xl_z & 0 & 0 & m_7l_z & m_8l_z \\ ml_z & 0 & 0 & 0 & ml_z{}^2 & -ml_xl_z & -m_7l_z & -m_8l_z & 0 & 0 \\ -ml_y & -ml_x & 0 & ml_xl_z & -ml_yl_z & m\left(l_x{}^2 + l_y{}^2\right) & m_7l_y & m_8l_y & m_7l_x & m_8l_x \end{bmatrix} \tag{18}$$

2.2.3. Cross-coupling force

The equation of motions of crane barge, hook, and shackle is summarized in a form of the second-order linear differential equations as Eq. (19).

$$\sum_{j=1}^{10}\left[\{m_{ij} + m_{ij}(\infty)\}\ddot{X}_j(t) + \int_{-\infty}^{t} L_{ij}(t-\tau)\dot{X}_j(\tau)d\tau + C_{ij}X_j(t)\right] = E_i(t) \tag{19}$$

where, m_{ij} is the generalized mass, $m_{ij}(\infty)$ the additional mass when frequency is infinite, $L_{ij}(t)$ the memory influence function, C_{ij} the restitution coefficient, $E_i(t)$ the wave-exciting force.

Since the hook and shackle constitute a double pendulum, the hook and shackle influence each other and induce irregular response even if regular external forces are acted. Therefore, the coupling equation as a function of time must be solved as an initial value problem.

First, $L_{ij}(t)$ on the left side of Eq. (19) can be obtained from Fourier transformation of the wave damping coefficient $B_{ij}(t)$.

$$L_{ij}(t) = \frac{2}{\pi}\int_0^{\infty} B_{ij}(\omega)\cos(\omega t)\,d\omega \tag{20}$$

Next, $E_i(t)$ is obtained by solving the integral equation based on the Green function in the time domain for the velocity potential under the boundary condition. The calculation of the Green function in the time domain requires a large amount of storage capacity and computation time; it is not suitable for analyzing the influence of the shape parameter of crane barge by changing its value. Therefore, in this study, by using the radiation velocity potential obtained in the process of calculating the memory influence function, the wave-exciting force is calculated by the Haskind relation (Takagi and Arai, 1996) from the radiation velocity potential.

Assuming that the impulse response function is $e_i(t)$ and the time series of the wave height is $h(t)$, the wave-exciting force $E_i(t)$ becomes Eq. (21).

$$E_i(t) = \int_{-\infty}^{t} h(t-\tau)e_i(\tau)d\tau \tag{21}$$

Here, $h(t)$ is the water surface variation of irregular wave estimated from the wave spectrum. Eq. (19) describes the equation of motions of crane barge at the origin O shown in *Fig. 3*; that is, $h(t)$ is the water surface variation at the origin. In this analysis, the irregular wave spectrum is given as Bretschneider spectrum.

The impulse response function, $e_i(t)$, is obtained from the Fourier transform of the response function $H_i(t)$ of the wave-exciting force as follows.

$$e_i(\tau) = Re[\frac{1}{2\pi} \int_{-\infty}^{\infty} H_i(\omega) e^{i\omega\tau} \, d\omega \,] \tag{22}$$

3. Hydraulic Experiments

3.1. Hydraulic experiments of crane barge motion (Nojiri and Mita, 1980)

First, the verification of the present coupling motion model of the crane barge, hook and shackle was carried out using the results obtained by Nojiri and Mita (1980). They measured the frequency response of a crane barge motion in a two-dimensional wave flume. *Table 1* shows the main specifications of the experiments.

The suspended load in their experiment is treated as a hook weight. *Figs. 7* and *8* show the comparison of the roll of crane barge and the hook swing angle respectively. The horizontal axis is the dimensionless frequency of the incident wave using the ship width B and gravity g, the vertical axis is the dimensionless amplitude of the hook swing angle divided by the wave slope (ka: k is the wave number, a is the wave amplitude). It is seen from the figures that the present numerical model gives good predictions of coupled motions of the crane barge and hook for roll and swing against all range of frequency with slight difference at the peak values.

Table 1: Main specifications of experiments

Item	Symbol	BARGE A	BARGE B
hull length	L (m)	2.470	2.470
hull width	B (m)	0.800	0.500
draft	d (m)	0.100	0.200
jib top coordinates	l_x (m)	0	0
	l_y (m)	0.425	0.425
	l_z (m)	0.750	0.650
hook weight	m (kg)	6.000	6.000
length of hanging	l (m)	0.408	0.300

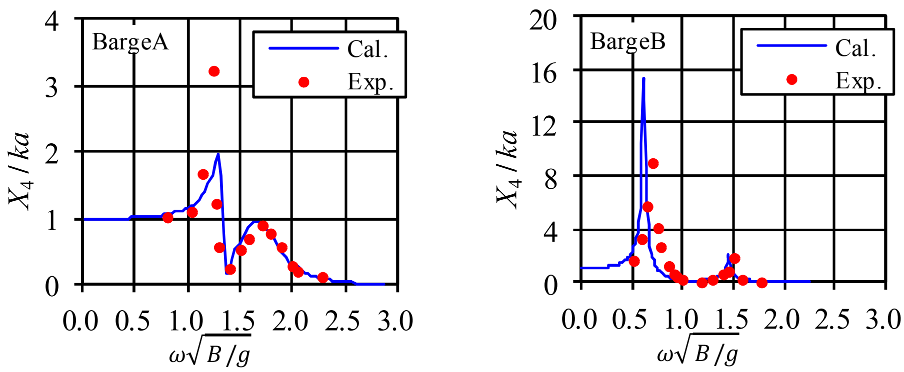

Figure 7: Comparison of the roll of crane barge

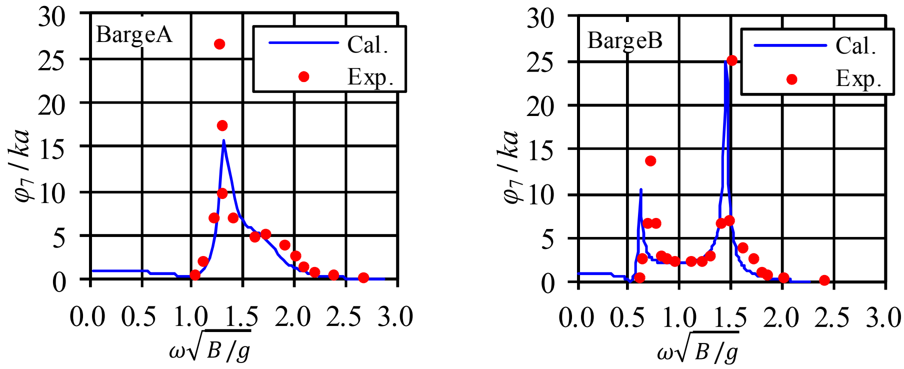

Figure 8: Comparison of the hook swing angle

3.2. Experiments of double pendulum motions

Next, to verify the present numerical model of the double pendulum motions of hook and shackle, laboratory experiments using an exciter was performed. A conceptual diagram and phots of the laboratory experiment are shown in *Fig. 9*.

In these experiments, the horizontal displacement of the jip, which is a fulcrum of a pendulum, was provided by an exciter (SSV-125, SANESU). The swing response of hook and shackle was measured. The motions of hook and shackle were measured with two video cameras (SSC-DC690, SONY) where the motions of light reflective markers attached to hook and shackle were taken and converted into displacement by image analysis.

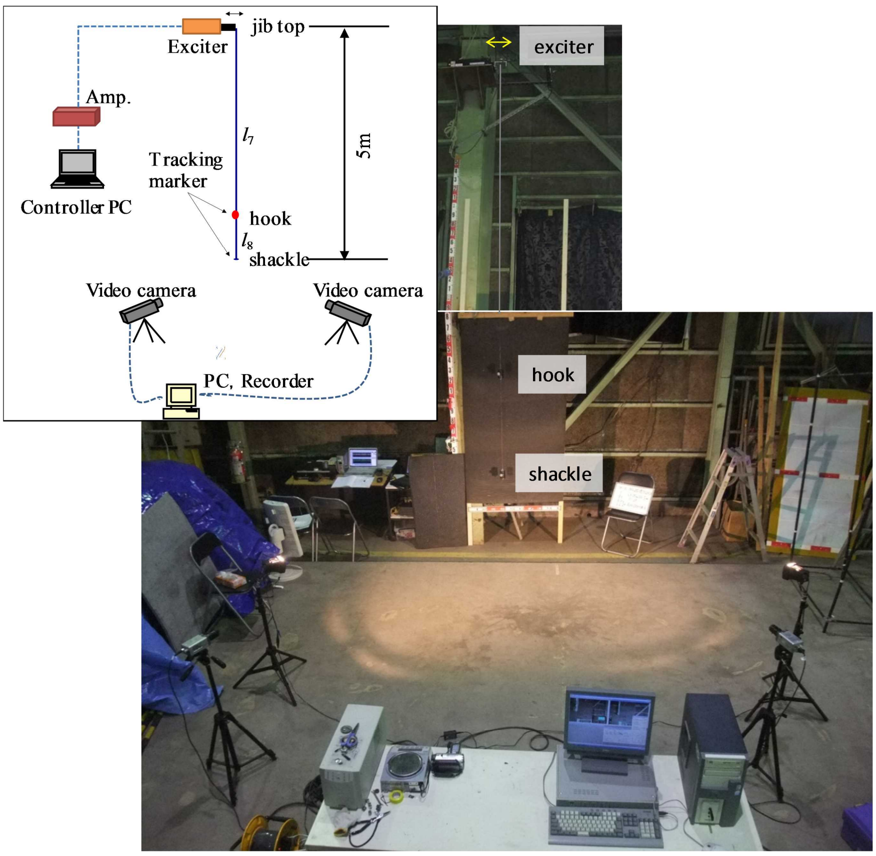

Figure 9: Conceptual diagram and phots of the laboratory motion experiments

The scale of experiments was 1/20, and the scaling was done according to Froude law. The exciter motion of the jib top was changed as two kinds of waveforms: a sinusoidal waveform and an irregular waveform exerted 50 waves or more. There were two experimental cases with different hanging lengths, as shown in *Table 2*. CASE-A is a reproduction of the construction work condition using a steel pipe pile by crane barge. Slingers connecting hook and shackle from jib top used in this experiment were synthetic polyvinylidene fluoride with low elongation at break.

The time series of motions of hook and shackle are shown in *Figs. 10* and *11*, respectively, when the jib top is subjected to sinusoidal excitations of 8 s period in the prototype scale. The vertical axis is the dimensionless swing amplitude normalized by the amplitude of the jib top motion. The predicted results agree well with the experimental data. The swing of hook has two peak periods of 8 s and 16 s in *Figs. 10* and *11*. Experimental motions seem to have a very long period trend compared to the calculated ones; this phenomenon is considered to be due to the influence of the longitudinal sling's vibration in the longitudinal direction, although slingers with low elongation at break were used.

The calculated value of shackle has the same swing amplitude and period trend as the experimental value; however, the amplitude is slightly smaller than the experimental value. In the calculation, the damping coefficient c_8 = 0.05 of the sling, determined from the measured swing amplitude of the shackle of the actual machine in sea waves, is considered. However, in the experiment, the shackle weight is m_8 = 0.003 kg and the estimated value of the damping coefficient c_8 is somewhat larger.

Table 2: Experimental cases of hanging length in protptype scale

		CASE-A		CASE-B	
		model	actual	model	actual
hook	length of hanging l_7 (m)	3.25	65.0	4.00	80.0
	weight m_7 (kg)	1.3	10,000	1.3	10,000
shackle	length of hanging l_8 (m)	1.25	25.0	0.50	10.0
	weight m_8 (kg)	0.003	20.0	0.003	20.0

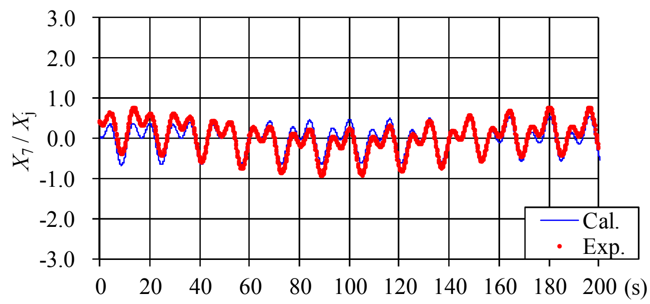

Figure 10: Time series of hook motion in regular excitation (CASE-A)

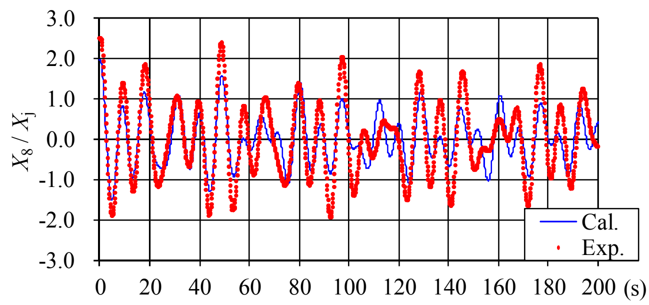

Figure 11: Time series of shackle motion in regular excitation (CASE-A)

Figure 12 shows a comparison between experimental and calculated significant swing amplitudes of hook and shackle when irregular excitation is applied to the jib top. The excitation direction of the jib top, simulating waves, is 45° with respect to the ship axis. The horizontal excitation displacement is given as 1 m corresponding to the incident significant wave height. The horizontal axis of *Fig. 12* is the incident significant wave period, and the vertical axis the significant swing amplitude X_s of the hook and shackle normalized by the significant excitation amplitude X_j of the jib top.

It is seen that in CASE-A the shackle oscillates around the hook with large amplitude of which ratio is from 8 to 10 at any periods. Those phenomena are well predicted by the present numerical model. It is also seen that the dimensionless hook and shackle motions are small in the range from 1.0 to 2.0, and predictions agree well with the experimental values.

By checking all experimental and calculated results, the validity of the present numerical model was ascertained for the crane barge motion and double pendulum motions of hook and shackle.

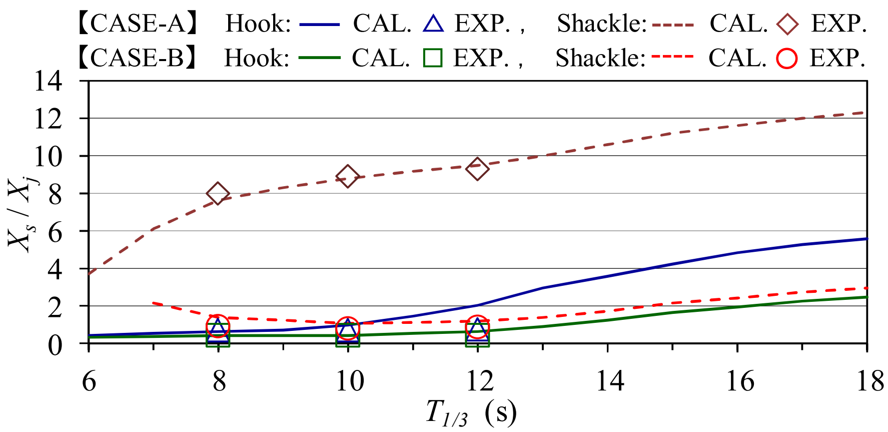

Figure 12: Dimensionless significant oscillation amplitude of hook and shackle in irregular excitation

4. Discussion

The proposed and validated numerical model was employed to investigate the oscillation characteristics of a crane barge, hook and shackle in waves. The analysis was conducted on a 1,600 tons crane barge (prototype size: L = 106 m, B = 43 m, d = 4.35 m). The hook and shackle were assumed to be suspended from the jib top of which position (l_x, l_y, l_z) = (50 m, 30 m, -95 m), and their weights were set to m_7 = 10 tons and m_8 = 0.02 tons.

Firstly, the frequency characteristics of jib top, hook and shackle motions in waves were investigated by spectral analysis. *Figure 13* shows the frequency spectra of jib top, hook and shackle motions in CASE-1 where the hook is located 25 m above the shackle and waves attack from 45° angle to the ship's *X* axis. The significant wave height and period are 1 m and 10 s, respectively. The natural oscillation periods of hook (T_7) and shackle (T_8) are summarized in *Table 3*, assuming that the righthand side of Eq. (2) is zero. As the position of the hook becomes lower, T_7 becomes short, and conversely, T_8 becomes long.

The jib-top motion spectrum has a peak around 0.1 Hz corresponding to the incident wave spectrum. On the other hand, the hook motion spectrum has a peak around 0.06 Hz on the low frequency side. The shackle motion spectrum has a sharp peak at 0.1 Hz and another peak around 0.06 Hz. Thus, it can be seen that each motion has different frequency characteristics.

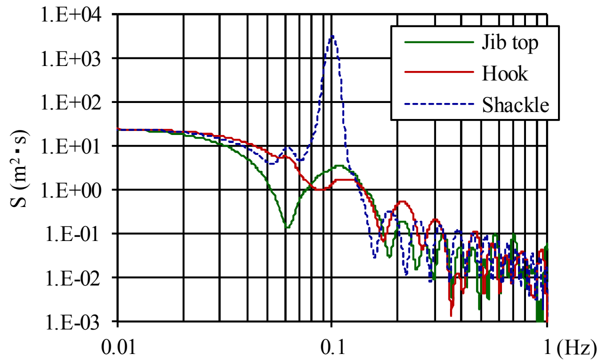

Figure 13: Frequency spectrum of jib top, hook, shackle motion

Subsequently, we examined the characteristics of shackle motion under the conditions that the position of shackle was the same (constant) and the hook was changed its position from 25 m to 5 m above the shackle at an interval of 5 m (denoted as CASE-1 to CASE-5). *Fig. 14* shows the dimensionless significant amplitude of shackle motion against the wave period when irregular wave incidence is 45° from the ship axis.

In the case that the hook is as high as 25 m above the shackle (CASE-1), the shackle is severely shaken by waves with 10 s period. The significant amplitude of this motion is 17 m. On the other hand, in the case of hysteresis of hook as low as 5 m above shackle (CASE-5), the oscillation is small and the significant amplitude is 1 m.

In CASE-1 to CASE-3, the peak of the shackle's significant amplitude largely appears to be around T_7. On the other hand, in CASE-4 to CASE-5, the peak of the shackle's significant amplitude appears to be on the long period around T_8. For waves with a wide range of periods seen in field ocean, if the natural periods T_7 and T_8 are close to each other, there is a high possibility that the oscillation of shackle will increase synchronously with the wave period. Therefore, if the distance between the hook and the shackle can be set so that the interval between T_1 and T_2 is large, the oscillation of the shackle can be reduced.

Table 3: Natural period of hook and shackle

	CASE-1	CASE-2	CASE-3	CASE-4	CASE-5
T_7 (s)	10.02	8.96	7.76	6.34	4.48
T_8 (s)	16.19	16.80	17.39	17.95	18.51

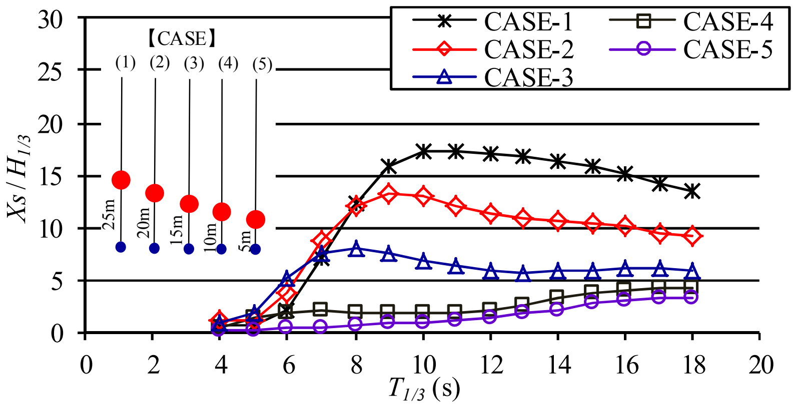

Figure 14: Dimensionless significant oscillation amplitude of shackle by changing hook position

Based on this finding, we actually measured the shaking motion by changing the distance between the hook and shackle from 6 m to 2 m, using a 200 tons crane barge as shown in *Fig. 15*. It is found that the significant amplitude of shackle oscillation could be reduced from 4.2 m to 1.9 m, which turns to be a 55% reduction.

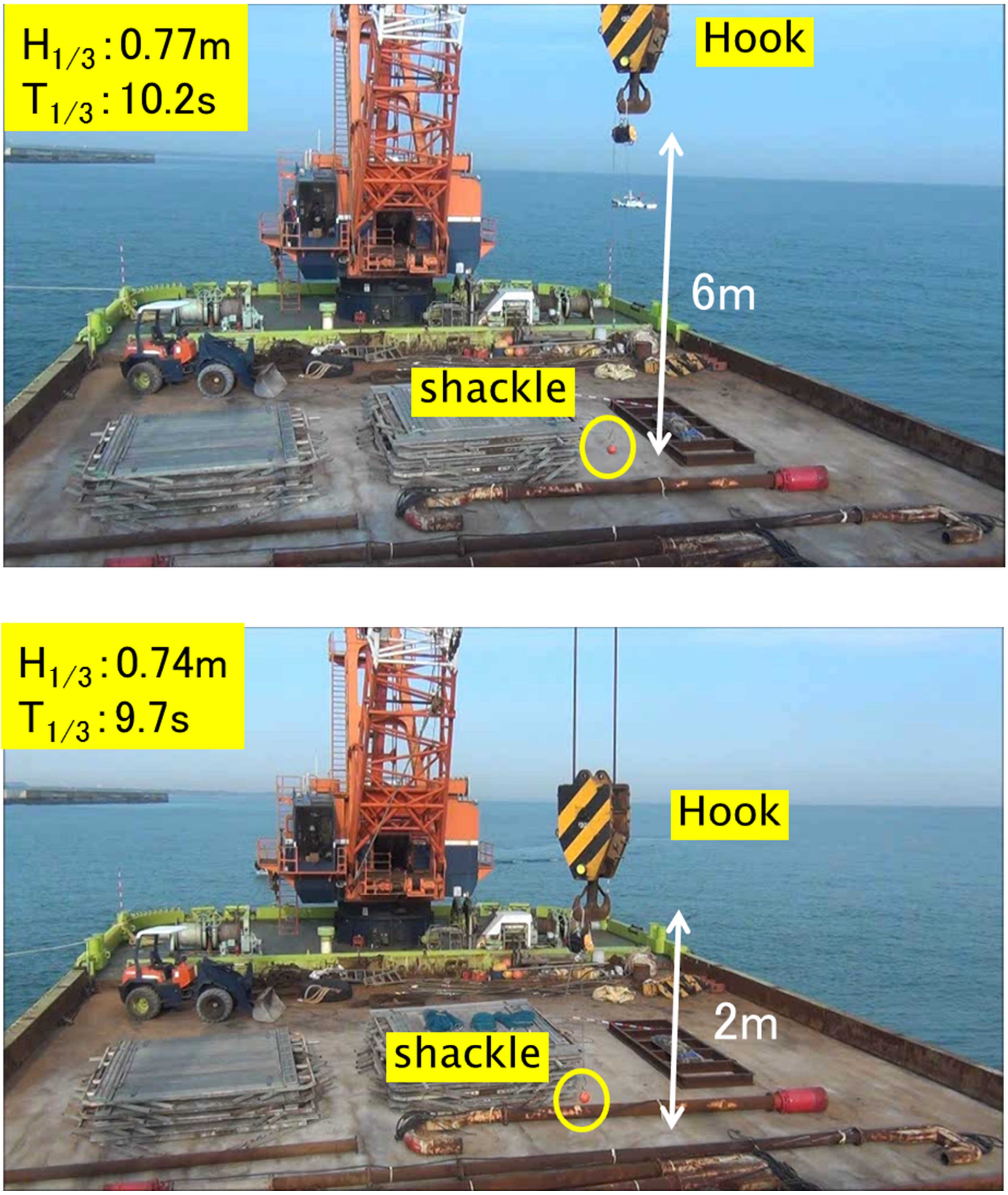

Figure 15: Field observation of hook and shackle motion hanged from a jib top of crane barge

5. Conclusions

We have developed a numerical model to analyse the cross-coupled motion between a crane barge in waves and a double pendulum consisted of hook and shackle. A set of experimental data was used to validate the model. The validated model is able to reproduce the swing motion of hook on a crane-barge. One of the objectives of the present study is how to reduce the swing motion of shackles using the numerical simulation model. The important conclusions of this study are summarized as follows.

1) The motion of shackle on a crane barge can be well predicted using the coupling model of motions proposed in this study.
2) The motion of shackle on a crane barge is larger than that of hook, and the motion of shackle is important in slinging work. The success or failure of slinging work significantly influences the rate of effective working days of maritime construction work.
3) When performing the slinging work, the swinging amplitude of shackle can be reduced by shortening the distance between the hook and shackle. This finding is especially important for the safety of marine construction work.

We believe that application of this research makes the development of accuracy and safety technologies in actual marine crane work.

6. Acknowledgments

The authors would like to thank to Dr. Hiroshi Kawabe belonging to Ship and Ocean Engineering Consultant Limited Liability Company for assistance with the numerical simulations and laboratory experiments.

References

Nojiri, N. and Mita, S. (1980): On the Coupled Motions between a Crane Barge and Hook Load in Wave, *Transactions of the West-Japan Society of Naval Architects*, Vol. 59, pp. 43-55.

Tsutsumi, T., Ogiwara, S., Jinnaka, T. (1974): On the principal particulars of ship hull form and wave pattern resistance (I). *Journal of the Society of Naval Architects of Japan*, Vol. 136, pp. 17-27.

Inglis, R. B. and Price, W. G. (1980): Comparison of Calculated Responses for Arbitrary Shaped Bodies using Two and Three-Dimensional Theories, *International Shipbuilding Progress*, Vol.27, No. 308, pp. 86-95.

Takagi, M. and Arai, S. (1996): Wave resistance theory of ships and marine structures, seizando-shoten publishing co.ltd, pp. 590-593.